

Retraction

Retracted: A Multiobjective Optimization Model for Prevention and Control of Coronavirus Disease 2019 in China

Discrete Dynamics in Nature and Society

Received 23 January 2024; Accepted 23 January 2024; Published 24 January 2024

Copyright © 2024 Discrete Dynamics in Nature and Society. This is an open access article distributed under the Creative Commons Attribution License, which permits unrestricted use, distribution, and reproduction in any medium, provided the original work is properly cited.

This article has been retracted by Hindawi following an investigation undertaken by the publisher [1]. This investigation has uncovered evidence of one or more of the following indicators of systematic manipulation of the publication process:

- (1) Discrepancies in scope
- (2) Discrepancies in the description of the research reported
- (3) Discrepancies between the availability of data and the research described
- (4) Inappropriate citations
- (5) Incoherent, meaningless and/or irrelevant content included in the article
- (6) Manipulated or compromised peer review

The presence of these indicators undermines our confidence in the integrity of the article's content and we cannot, therefore, vouch for its reliability. Please note that this notice is intended solely to alert readers that the content of this article is unreliable. We have not investigated whether authors were aware of or involved in the systematic manipulation of the publication process.

Wiley and Hindawi regrets that the usual quality checks did not identify these issues before publication and have since put additional measures in place to safeguard research integrity.

We wish to credit our own Research Integrity and Research Publishing teams and anonymous and named external researchers and research integrity experts for contributing to this investigation.

The corresponding author, as the representative of all authors, has been given the opportunity to register their agreement or disagreement to this retraction. We have kept a record of any response received.

References

- [1] X. Li, Z. Liu, and F. Ge, "A Multiobjective Optimization Model for Prevention and Control of Coronavirus Disease 2019 in China," *Discrete Dynamics in Nature and Society*, vol. 2022, Article ID 6329601, 10 pages, 2022.

Research Article

A Multiobjective Optimization Model for Prevention and Control of Coronavirus Disease 2019 in China

Xiaocheng Li ¹, Zhaoli Liu,¹ and Fangzhen Ge²

¹School of Mathematical Sciences, Huaibei Normal University, Huaibei 235000, China

²School of Computer Science and Technology, Huaibei Normal University, Huaibei 235000, China

Correspondence should be addressed to Xiaocheng Li; mathlxc@chnu.edu.cn

Received 15 November 2021; Accepted 18 December 2021; Published 5 January 2022

Academic Editor: Gengxin Sun

Copyright © 2022 Xiaocheng Li et al. This is an open access article distributed under the Creative Commons Attribution License, which permits unrestricted use, distribution, and reproduction in any medium, provided the original work is properly cited.

It is a global issue to set up a practical, sensitive, and useful model to eradicate or mitigate the coronavirus disease 2019 (COVID-19). Taking Central China's Hubei Province for example, three models were established. Firstly, a susceptible-probable-infectious-recovered (SPIR) model was proposed to predict the monthly number of confirmed and susceptible cases in each city. Next, an epidemic prefecture clustering model was set up to find proper vaccine delivery sites, according to the distance of each city. Finally, a dynamic material delivery optimization model was established for multiple epidemic prefectures, aiming to speed up vaccine production and storage in each delivery site.

1. Introduction

Coronavirus disease 2019 (COVID-19) is a serious and fatal disease, which threatens the public health of the entire world. Some susceptible cases were found in Wuhan, China, as early as December 2019 [1]. On January 12, 2020, the World Health Organization (WHO) named this highly contagious disease 2019-novel coronavirus (2019-nCoV) [2] and announced that the disease has no specific medicine, but routine antiviral treatment. Therefore, it is a global issue to set up a practical, sensitive, and useful model to eradicate or mitigate the disease. Otherwise, COVID-19 will upgrade and spread like Ebola, put the fundamental survival of the society at stake, and might even paralyze countries. China's experience in upgrading personal protective equipment, building mobile labs, mobilizing medical staff, and real-time tracking of epidemic spread has played an important role in COVID-19 prevention and control [3].

Li and Bai [4] established an infectious disease model constrained by nonlinear incidence and maximum treatment capacity. Comparing recent cumulative and predicted cases, Kumar and Bhagavathula [5] forecasted that the confirmed cases, deaths, and recoveries will double in all the observed countries except China, Switzerland, and

Germany, and the death and recovery rates will increase faster than confirmed cases in the next two months. Augusto [6] modeled the transmission dynamics of Ebola with relapse and reinfection and discovered that high efficacy control measures can effectively curtail Ebola in the community. Yi et al. [7] proved that the joint prevention between the government, the masses, and hospitals is a scientific way to prevent and control the epidemic, using the five-early model (early detection, early screening, early diagnosis, early quarantine, and early recovery). Kennedy et al. [8] suggested that the magnitude and duration of social distancing required to control the pandemic can be reduced, if people exercise caution in public by protecting themselves. Using the S(usceptible) U(nidentified infectious) I(dentified infectious) H(ospitalized) R(ecovered) model (SUIHR), Zhen et al. [9] justified the extremely strict border control in entities of China. Rui and Tian [10] divided the population into susceptible, infective, recovered, and dead populations and then reveal the law of epidemic transmission by the SIRD model. Wu et al. [11] established a generalized-growth model to present the evolution of the number of the total confirmed cases changing with time.

In the light of the above, this article aims at modeling COVID-19 trend based on factors such as spread rate,

vaccine demand, delivery site, and vaccine production rate, to name but a few, and optimize the model by bringing in other key factors. Specifically, three models were established to provide the optimal scheme to allay the severe COVID-19 epidemic. Firstly, the susceptible-probable-infectious-recovered (SPIR) model was employed to predict the situation at the outbreak of the disease. Then, the k-means clustering (KMC) model [12–14] was introduced to optimize the delivery sites of vaccines and medical staff. Finally, a dynamic material delivery optimization model was constructed to deliver sufficient vaccines and medical staff in the shortest time and at the minimum cost. Figure 1 is the roadmap of this research.

2. Hypotheses and Symbols

2.1. Hypotheses

H1: the objects form an ideal, uniformly mixed group. The total number of objects remains at N , without death caused by immigration, emigration, or other reasons.

H2: those infected with COVID-19 will eventually recover and acquire long-term immunity through treatment.

H3: the infected are immediately contagious, because COVID-19 is mildly infectious, despite its long incubation period.

H4: the objects are divided into four classes: the susceptible, the probable, the infected, and the removed.

H5: once the epidemic breaks out in a prefecture, the prefecture will be immediately quarantined, cutting off the flow of population.

H6: the storages f emergency materials in each prefecture have enough vehicles to deliver the materials in time.

2.2. *Symbols.* The main variables involved in this article are shown in Table 1.

3. COVID-19 Modeling

According to China's National Health Commission (NHC), the nationwide distribution of COVID-19 epidemic on February 1, 2020, was obtained. The number of COVID-19 cases in Chinese provinces is shown in Figure 2.

As shown in Figure 2, Hubei, Zhejiang, and Guangdong led the country in terms of the number of COVID-19 cases. The number of infected people in Hubei province accounted for 63.1 percent of the total, higher than any other province in China. Therefore, Hubei was taken as an example in our research.

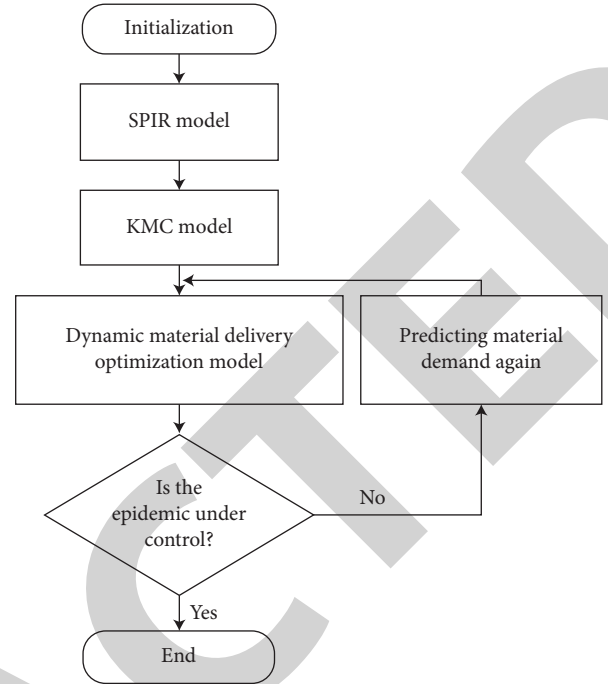


FIGURE 1: Research roadmap.

3.1. *Models.* As mentioned before, the objects form an ideal, uniformly mixed group. The total number of objects remains at N , without death caused by immigration, emigration, or other reasons. The objects were divided into four groups: the susceptible S , the probable P , the infected I , and the removed R . Figure 3 shows the relationship between the four groups.

The traditional susceptible, infected, recovered (SIR) model [15–18] can be expressed as

$$\begin{cases} \frac{di}{dt} = \lambda si - \mu i, & i(0) = i_0, \\ \frac{ds}{dt} = -\lambda si, & s(0) = s_0, \\ \frac{dr}{dt} = \mu i, & r(0) = r_0, \end{cases} \quad (1)$$

where i is the number of the infected person, s is the number of the susceptible person, r is the number of the recovered person, and μ is the recovered ratio.

3.2. *Models Optimization.* The transmission mechanism of COVID-19 differs from that of general infectious diseases, which involve the normally infected, patients, and the removed. COVID-19 has an additional group of objects: the susceptible. This group has similar symptoms with COVID-19, but cannot be diagnosed as infected with COVID-19 or general flus. Some of these objects might be transformed into

TABLE 1: Symbols of key variates.

Symbol	Unit	Description
N	Person	Total population
$s(t)$	%	Percentage of the infected at time t in the total population
$i(t)$	%	Percentage of patients at time t in the total population
$e(t)$	%	Percentage of the susceptible at time t in the total population
$r(t)$	%	Percentage of the recovered at time t in the total population
θ_1	%	Percentage of the susceptible diagnosed as normally infected per day
θ_2	%	Percentage of the susceptible diagnosed as infected per day
h	%	Remove ratio (the sum of death rate and recover rate per day)
λ	Person	Daily contracting ratio (the mean number of people infected by a patient through contact)
C_i	\$	Fixed cost of setting up i storages
C_s	\$	Subsidy of medical staff
C_d	\$	Transport cost of each dose per unit of distance
t_{ij}	day	Travel time from i to j
T_k	day	Time threshold of vaccine delivery (violating the threshold will bring a penalty cost)
M_{ij}	Dose	Quantity of vaccines delivered from i to j
X_{ij}	km	Distance between i and j
D_j	Dose	Vaccine demand of j
N_{ij}	Group	Number of medical groups delivered from i to j
β	—	Ratio of the infected to medical staff
I	Person	Number of the infected
V_0	km/h	Vaccine delivery speed from storages to the epidemic prefecture
V^p	Dose/day	Vaccine production speed
Y_{ij}	Person	Number of medical staff delivered from i to j
S_i	Dose	The drug storage capacity of the i -th inventory point

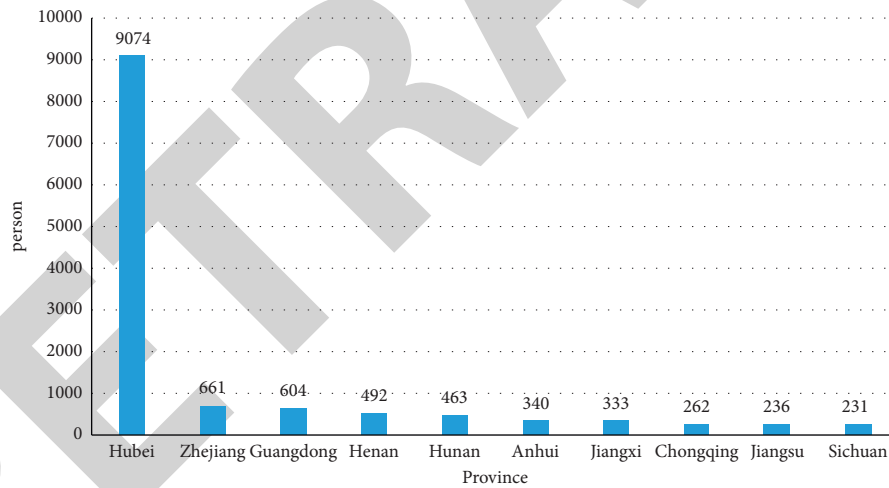


FIGURE 2: Top 10 provinces by the number of COVID-19 cases.

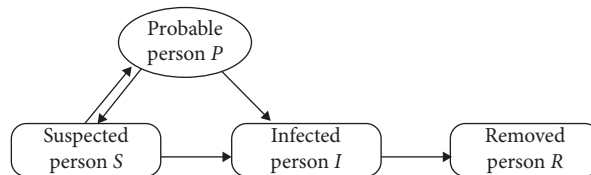


FIGURE 3: Relationship between different groups.

patients or normally infected. Hence, the susceptible was added to the traditional SIR model:

$$\begin{cases} s + p + i + r = 1, \\ \frac{ds}{dt} = \theta_1 p - \lambda si, \quad s(0) = s_0, \\ \frac{di}{dt} = \lambda si - hi + \theta_2 p, \quad i(0) = i_0, \\ \frac{dr}{dt} = hi, \quad r(0) = r_0, \\ \frac{de}{dt} = -\theta_1 p - \theta_2 p, \quad e(0) = e_0. \end{cases} \quad (2)$$

3.3. Parameter Evaluation. The above model contains the following key parameters: percentage of the susceptible diagnosed as normally infected θ_1 per day; percentage of the susceptible diagnosed as infected θ_2 per day; and the sum of death rate and recover rate per day (remove ratio) h . The values of these parameters can be approximated according to the official data released each day:

$$\begin{aligned} \theta_1 &= \frac{\text{newly added removal of suspected per day}}{\text{total suspected on the current day}}, \\ \theta_2 &= \frac{\text{newly added transformation of susceptible to patients per day}}{\text{total susceptible on the current day}}, \\ h &= \frac{\text{newly added recovered and deaths per day}}{\text{total susceptible on the current day}}. \end{aligned} \quad (3)$$

By our research hypotheses, the contracting probability of two persons is closely related to the population size. Therefore, it is assumed that the effective contracting ratio is the reciprocal of the population, $\lambda = 1/N$.

3.4. Model Solution. The epidemic severity in Hubei varies from prefecture to prefecture. It is necessary to optimize the material delivery sites for the province [19]. Before that, the number of COVID-19 patients should be predicted for each prefecture.

As shown in Figure 4, from 31 December 2019 to 1 February 2020, Wuhan had more infected than any other prefecture in Hubei. Several other prefectures also faced a serious epidemic: Huanggang, Xiaogan, Jingzhou, Ezhou, Suizhou, and Huangshi. In the said period, Wuhan and Jingzhou were the epicenters of the epidemic. Hence, this subsection attempts to predict the COVID-19 situation in each prefecture of Hubei with the SPIR model. However, it is impossible to directly drive S, P, I, and R values with the SPIR model. To solve this problem, the Runge–Kutta method of MATLAB was called to obtain these solutions [21, 22]. And in the Runge–Kutta method, the initial value of parameters, θ_1 , θ_2 , h , and λ , are set as 0.001, 0.001, 0.0001, and 0.001, respectively.

The key parameters for Hubei were solved by differential equations (2). The solutions are given in Table 2. Then, the COVID-19 cases in the next month were predicted.

Figure 5 shows the number of diagnosed patients in Hubei. It can be seen that the epidemic reached its peak in the 10th week after the outbreak, as the patients took up 0.035% of the total population. In the 28th week, the epidemic was under control, when the percentage of patients dropped to 0.

3.5. Results and Analysis. The above model was applied to predict the COVID-19 situation of other preferences in four weeks. The results are given in Tables 3 and 4.

4. KMC Model

Under the condition of ensuring the safety of the epidemic, in order to quickly transport medical workers, medical supplies, and related materials to the affected areas, Hubei was divided into three regions according to the geographical coordinates of the cities and airports. For each region, a material delivery site was established [23, 24]. Once the epidemic breaks out, the local site will transfer vaccines and medical staff to the affected prefectures. If the local force is



FIGURE 4: Epidemic distribution in Hubei [20].

TABLE 2: Values of key parameters.

Parameters	θ_1	θ_2	h	λ
Values	0.0035	0.0037	0.0003	0.00017

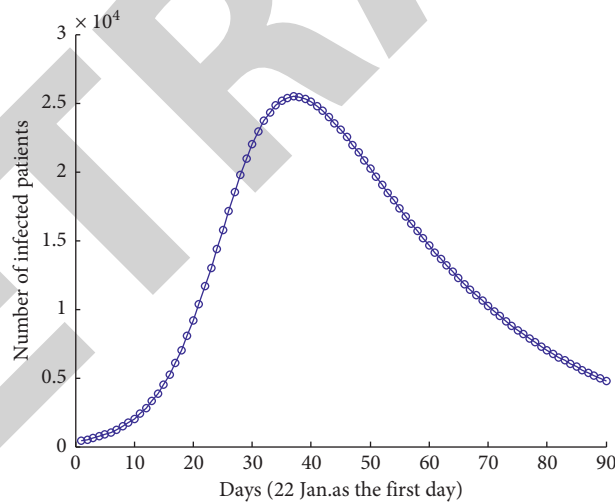


FIGURE 5: Number of patients over time.

insufficient to control the epidemic, the other prefectures will transfer vaccines and medical staff to this prefecture.

4.1. KMC. The distance from point i to point j can be defined as

$$d_{ij}(q) = \left[\sum_{k=1}^p |x_{ik} - x_{jk}|^q \right]^{1/q} \tag{4}$$

If $q = 2$, then the Euclidean distance $d_{ij}(2) = \left[\sum_{k=1}^p (x_{ik} - x_{jk})^2 \right]^{1/2}$.

The general steps of KMC [25, 26] are given in Figure 6:

- Step 1: select a number of sample points as cluster heads by experience or basic knowledge of data
- Step 2: compute the Euclidean distance between each sample point and each cluster head, and allocate the sample point to the cluster of the nearest cluster head
- Step 3: classify one sample point at a time, and compute the mean of each cluster to update the cluster head
- Step 4: repeat Step 2 with the new cluster head, and classify the sample points again

TABLE 3: Predicted new susceptible in four weeks.

Prefecture	Week				Total
	1	2	3	4	
Wuhan	1008.2	4035.7	8658.8	12510.4	26213.1
Huanggang	66.8	212.4	604.4	878.6	1762.1
Xiaogan	78.0	244.5	576.3	1045.7	1944.5
Xiangyang	26.4	91.0	257.3	335.2	709.9
Suizhou	31.6	88.4	248.6	336.8	705.5
Yichang	23.2	68.5	185.5	239.1	516.3
Jingzhou	34.6	114.3	304.6	492.0	945.5
Jingmen	24.8	68.8	209.6	249.3	552.5
Ezhou	29.6	88.1	280.5	362.0	760.1
Huangshi	25.8	67.8	219.5	252.2	565.2
Xianning	17.2	57.0	175.3	229.6	479.0
Shiyan	15.8	45.5	123.5	156.5	341.3
Xiantao	14.0	45.7	116.3	168.4	344.3
Enshi	5.0	18.1	44.7	72.9	140.6
Tianmen	9.3	33.2	88.0	121.2	251.6
Qianjiang	4.6	16.9	39.4	59.0	120.0
Shennongjia	0.3	0.9	2.1	3.4	6.6

TABLE 4: Predicted new patients in four weeks.

Prefecture	Week			Total
	1	3	4	
Wuhan	789.9	6506.6	9392.1	19341
Huanggang	45.1	371.8	536.7	1105.1
Xiaogan	55.1	453.5	654.6	1347.9
Xiangyang	18.8	155.0	223.7	460.7
Suizhou	20.0	164.7	237.7	489.5
Yichang	14.7	121.0	174.7	359.8
Jingzhou	25.5	210.2	303.4	624.9
Jingmen	16.0	132.1	190.7	392.8
Ezhou	21.0	172.7	249.2	513.2
Huangshi	16.0	131.9	190.4	392.0
Xianning	13.1	108.1	156.1	321.4
Shiyan	10.3	84.8	122.4	252.0
Xiantao	8.9	73.2	105.6	217.5
Enshi	3.9	31.7	45.8	94.4
Tianmen	7.2	59.0	85.1	175.3
Qianjiang	3.1	25.6	36.9	75.9
Shennongjia	0.2	1.4	2.0	4.2

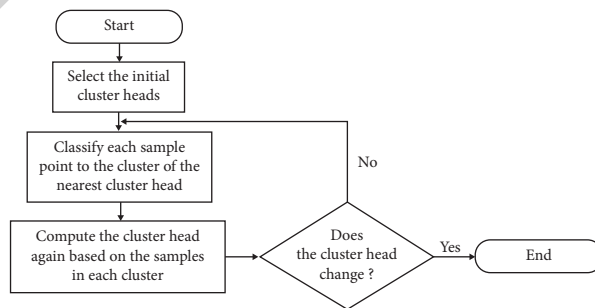


FIGURE 6: Flow of KMC.

Step 5: repeat Steps 2–4 cyclically and adjust the classes until no cluster head changes to obtain the final classes

4.2. *Solution of the Model.* Table 5 sums up the coordinates of the central cities of the prefectures in Hubei.

According to the clustering results, Hubei was divided into three regions. The first region includes Yichang, Jingzhou, and Enshi; the second contains Wuhan, Huanggang, Xiaogan, Suizhou, Ezhou, Huangshi, Xianning, Xiantao, Tianmen, and Qianjiang; and the third covers Xiangyang, Jingmen, Shiyan, and Shennongjia.

The coordinates of the head of each cluster were solved and taken as the location of the delivery site in the corresponding region, because the head is the closest point to any sample point in the cluster. The coordinates of the three heads were Yichang (8.31, 2.28), Wuhan (21.83, 2.04), and Xiangyang (11.54, 9.84).

5. Dynamic Material Delivery Optimization Model

By Model 1, it is possible to predict the number of patients in each prefecture in the near future and determine the newly added patients according to the distribution of the infected. From the perspective of emergency rescue, the number of patients and the growth of the infected must be suppressed by sufficient supply of vaccines. This is the only way to effectively control the epidemic [27, 28].

Based on SPIR model, this article establishes a dynamic emergency delivery optimization model for multiple epidemic prefectures [29, 30]. The model has two objective functions: the minimum delivery time $F_1(t)$ and the minimum transport cost $F_2(t)$.

5.1. Objective Functions

5.1.1. *Minimum Delivery Time.* Considering the high death rate of COVID-19, vaccines and medical staff should be delivered as soon as possible, that is, within the threshold of the arrival time. Otherwise, the severity and scope of the epidemic will go out of control. The penalty cost incurred by the violation of the threshold of the arrival time can be described as an exponential function:

$$\min F_1(t) = e^{\max\{0, t_{ij} - T_k\}}. \quad (5)$$

5.1.2. *Minimum Transport Cost.* Besides delivery time, the transport cost must also be minimized to deliver vaccines and medical staff to the epidemic prefecture. The transport cost covers delivery cost, staff salary, and storage cost:

$$\min C(t) = \sum_{i=1}^m \sum_{j=1}^n (C_d X_{ij} M_{ij} + C_s Y_{ij}) + C_0, \quad (6)$$

where C_0 is the total fixed cost of setting up i storages; C_s is the subsidy of each medical staff member; C_d is the transport cost of a dose per unit distance; Y_{ij} is number of

TABLE 5: Coordinates of central cities of the prefectures in Hubei.

Prefecture	x	y
Wuhan	21.83	2.04
Huanggang	24.87	1.75
Xiaogan	20.00	3.94
Xiangyang	11.54	9.84
Suizhou	17.49	8.20
Yichang	8.31	2.28
Jingzhou	12.51	0.29
Jingmen	11.91	4.02
Ezhou	24.26	1.16
Huangshi	25.61	0
Xianning	22.20	-2.12
Shiyan	5.66	12.96
Xiantao	18.10	0.45
Enshi	0	0
Tianmen	16.91	2.25
Qianjiang	15.45	0.79
Shennongjia	4.76	8.07

medical staff delivered from i to j ; M_{ij} is the quantity of vaccines delivered from i to j ; and X_{ij} is the distance between i and j .

5.1.3. *Composite Objective Function.* The dynamic material delivery optimization model has two objective functions: the minimum delivery time $F_1(t)$ and the minimum transport cost $F_2(t)$. The two functions need to be normalized to unify their dimensionality:

$$\begin{aligned} \min \overline{F_1(t)} &= \frac{F_1(t) - F_1(t)_{\min}}{F_1(t)_{\max} - F_1(t)_{\min}}, \\ \min \overline{F_2(t)} &= \frac{F_2(t) - F_2(t)_{\min}}{F_2(t)_{\max} - F_2(t)_{\min}}, \end{aligned} \quad (7)$$

where $F_1(t)_{\max}$ and $F_1(t)_{\min}$ are the maximum and minimum expectations of $F_1(t)$, respectively, and $F_2(t)_{\max}$ and $F_2(t)_{\min}$ are the maximum and minimum expectations of $F_2(t)$, respectively.

Since two objectives have different priorities, weight coefficients were introduced to combine them into one composite objective function, turning the multiobjective optimization problem into a single-objective optimization problem:

$$\min F(t) = \alpha \overline{F_1(t)} - (1 - \alpha) \overline{F_2(t)}, \quad \alpha \in (0, 1). \quad (8)$$

5.2. Constraints

5.2.1. *Vaccine Demand.* To control epidemic dissemination, the vaccine demand of each epidemic prefecture must be satisfied by the sum of vaccines and medical staff delivered to that prefecture:

$$\sum_{i=1}^m M_{ij} = D_j, \quad i = 1, 2, 3, \dots, m; j = 1, 2, 3, \dots, n. \quad (9)$$

5.2.2. *Vaccine Supply.* Practically, it is impossible to deliver an infinite number of materials to epidemic prefectures. The total vaccines transferred from storage i to each epidemic prefecture should not surpass the vaccine supply capability:

$$\sum_{j=1}^n M_{ij} \leq S_i, \quad i = 1, 2, 3, \dots, m; j = 1, 2, 3 \dots n. \quad (10)$$

Every medical staff member involved in the rescue mission must be trained professionally, as medical staff have the highest infection rate of COVID-19 among all groups of people. According to the Health Commission of Hubei Province, there are a total of 54 million medical staff that could support the epidemic control in Hubei. This number should not be exceeded by the total medical staff delivered to epidemic prefectures. Let N_{ij} be a group of eight medical staff. In addition, there is a correspondence between medical staff groups and the infected: one group is needed to treat every 15 infected. The two numbers should grow in proportionality. If not, the rounding-plus-one method was adopted to confirm the number of groups:

$$\begin{aligned} \sum_{i=1}^m \sum_{j=1}^n Y_{ij} &\leq 540000, \\ Y_{ij} &= 8N_{ij}, \\ N_{ij} &= \begin{cases} \beta I, & \beta I \in N^+, \\ [\beta I] + 1, & \beta I \notin N^+. \end{cases} \end{aligned} \quad (11)$$

5.2.3. *Arrival Time.* The period from the epidemic outbreak to the arrival of vaccines and medical staff at the epidemic prefecture covers the following stages: the period from vaccine production to delivery at each storage; the period for vaccines and medical staff to move from the storage to the epidemic prefecture; and the response period of the emergency system to the epidemic:

$$t_{ij} = \frac{X_{ij}}{V_0} + \sum_{i=1}^m \sum_{j=1}^n \frac{M_{ij}}{V_p} + t_0, \quad (12)$$

$$\min F_1(t) = 0.8\overline{F_1(t)} + 0.2\overline{F_2(t)},$$

$$\left. \begin{aligned} &\sum_{i=1}^m M_{ij} = D_j, \quad i = 1, 2, 3, \dots, m; j = 1, 2, 3 \dots n, \\ &\sum_{j=1}^n M_{ij} \leq S_i, \quad i = 1, 2, 3, \dots, m; j = 1, 2, 3 \dots n, \\ \text{s.t.} &\sum_{i=1}^m \sum_{j=1}^n Y_{ij} \leq 4116, \\ &M_{ij} \geq 0, \\ &t_{ij} = \frac{X_{ij}}{V_0} + \sum_{i=1}^m \sum_{j=1}^n \frac{M_{ij}}{V_p} + t_0. \end{aligned} \right\} \quad (13)$$

TABLE 6: Value of each key parameter.

Parameters	C_0	C_d	C_s	T_k
Value	3200	4.725	100	2.5

TABLE 7: Distance between prefectures and delivery sites.

Prefecture	Site		
	Yichang	Wuhan	Xiangyang
Wuhan	288.91	0	257.99
Huanggang	344.57	57.05	311.79
Xiaogan	253.23	51.59	206.9
Xiangyang	168.31	257.99	0
Suizhou	228.69	152.67	119.86
Yichang	0	288.91	168.31
Jingzhou	99.81	200.52	187.95
Jingmen	95.11	206.03	110.11
Ezhou	346.1	59.81	315.77
Huangshi	363.49	82.89	340.53
Xianning	306.64	83.36	317.67
Shiyan	221.79	403.47	146.45
Xiantao	210.9	85.31	221.1
Enshi	178.91	463.85	318.53
Tianmen	180.64	108.32	178.53
Qianjiang	156.23	137.41	190.85
Shennongjia	130.28	368	142.83

where t_0 is the response period of the system; V_p is the vaccine production speed; and V_0 is the delivery speed from storage to epidemic prefecture.

5.3. *Solution of the Model.* Referring to epidemic situations in previous years [31], the values of key parameters can be obtained as shown in Table 6.

With $\alpha = 0.8$, the dynamic material delivery optimization model can be expressed as

TABLE 8: The drug distribution scheme.

	Vaccine quantity
S1-Jingzhou	1840
S1-Enshi	720
S2-Huanggang	11040
S2-Xiaogan	4840
S2-Suizhou	3200
S2-Ezhou	2040
S2-Huangshi	1720
S2-Xianning	1600
S2-Xiantao	1720
S2-Tianmen	680
S2-Qianjiang	320
S3-Jingmen	3120
S3-Shiyan	1400
S3-Shennongjia	0

TABLE 9: Medical staff delivery scheme.

	Number of medical staff
S1-Jingzhou	30
S1-Enshi	12
S2-Huanggang	180
S2-Xiaogan	79
S2-Suizhou	52
S2-Ezhou	33
S2-Huangshi	28
S2-Xianning	26
S2-Xiantao	28
S2-Tianmen	11
S2-Qianjiang	5
S3-Jingmen	51
S3-Shiyan	23
S3-Shennongjia	0

The distance between prefectures and delivery sites is shown in Table 7.

Through LINGO modeling, the optimal vaccine distribution scheme was obtained (Table 8). The vaccine quantities delivered from the three sites were $S1 = 2560$, $S2 = 27160$, and $S3 = 4520$.

The vaccine production speed was $V_p = \sum_{i=1}^m \sum_{j=1}^m M_{ij}/t_0 = 34240/28 \approx 1223$ doses/day.

Then, the number of medical staff delivered from the three sites to each epidemic prefecture was calculated (Table 9). The coordinates of the three delivery sites were S1 (8.31, 2.28), S2 (21.83, 2.04), and S3 (11.54, 9.84).

6. Conclusions

Based on the characteristics of the spread of COVID-19 and treatment procedures, three models of organic linkage were established to address the epidemic prevention and control issues systematically. The results reflect the stability and reliability of our models.

Model 1 considers the driving effect of COVID-19 diffusion on the distribution of materials and the inverse control of material flow on disease spread. The modeling

results are reasonable and practical, because various factors were coupled with the SPIR infectious diseases model.

Model 2 relies on KMC to cluster the epidemic prefectures by the Euclidean distance. The modeling results lay the basis for optimizing the material delivery of Model 3 and help to choose the best delivery sites.

Model 3 takes account of the competition between epidemic prefectures for medical resources, and the distance between epidemic prefecture and delivery site, as well as the severity of the epidemic. In this way, the authors derived a practical distribution scheme for emergency materials.

Data Availability

The data used to support the findings of this study are available from the corresponding author upon request.

Conflicts of Interest

The authors declare that they have no conflicts of interest.

Acknowledgments

This work was supported by the Natural Science Foundation of Anhui Province, China (Grant no. 1808085MF174).

References

- [1] H. Allahverdipour, "Battle against novel coronavirus 2019-nCoV: international commitment to develop worldwide informing campaigns," *Health Promotion Perspectives*, vol. 10, no. 2, p. 94, 2020.
- [2] G. Al and D. Akash, "Novel coronavirus COVID-19: an overview for emergency clinicians," *Emergency Medicine Practice*, vol. 22, no. 2, pp. 1-21, 2020.
- [3] Y. H. Zhang, S. Wang, and Y. Q. Chen, "Study on Ebola hemorrhagic fever and the disease progress in 2014," *Infectious Disease Information*, vol. 4, pp. 3-8, 2014.
- [4] G. H. Li and J. Bai, "The study on an epidemic model with nonlinear incidence and piecewise treatment function," *Mathematics in Practice and Theory*, vol. 44, no. 21, pp. 228-236, 2014.
- [5] S. R. Kumar and R. M. Bhagavathula, "Prediction of the COVID-19 pandemic for the Top 15 affected countries: advanced autoregressive integrated moving average (ARIMA) model," *JMIR Public Health and Surveillance*, vol. 6, no. 2, Article ID e19115, 2020.
- [6] F. B. Agosto, "Mathematical model of Ebola transmission dynamics with relapse and reinfection," *Mathematical Biosciences*, vol. 283, no. 1, pp. 48-59, 2017.
- [7] Q. J. Yi, W. Fang, and C. H. Lang, "Five-early model: the magic weapon against COVID-19," *Iranian Journal of Public Health*, vol. 49, no. Z1, pp. 82-86, 2020.
- [8] D. M. Kennedy, G. J. Zambrano, and Y. Y. Wang, "Modeling the effects of intervention strategies on COVID-19 transmission dynamics," *Journal of Clinical Virology: the Official Publication of the Pan American Society for Clinical Virology*, vol. 128, no. 7, Article ID 104440, 2020.
- [9] Z. Zhen, W. Enzo, and S. Till, "Sustainable border control policy in the COVID-19 pandemic: a math modeling study," *Travel Medicine and Infectious Disease*, vol. 41, no. 5, Article ID 102044, 2020.

- [10] R. Rui and M. Tian, "Joint estimation of case fatality rate of COVID-19 and power of quarantine strategy performed in Wuhan, China," *Biometrical Journal*, vol. 63, no. 1, pp. 46–58, 2021.
- [11] Y. Wu, L. Zhang, and W. J. Cao, "The generalized-growth modeling of COVID-19," *Frontiers in Physics*, vol. 8, Article ID 603001, 2021.
- [12] S. Tuncer and A. Alkan, "Spinal cord based kidney segmentation using connected component labeling and K-means clustering algorithm," *Traitement du Signal*, vol. 36, no. 6, pp. 521–527, 2019.
- [13] H. Thottathyl, K. K. Pavan, and R. P. Panchadula, "Microarray breast cancer data clustering using map reduce based K-means algorithm," *Revue d'Intelligence Artificielle*, vol. 34, no. 6, pp. 763–769, 2020.
- [14] A. Saglam, H. B. Makineci, Ö. K. Baykan, and N. A. Baykan, "Clustering-based plane refitting of non-planar patches for voxel-based 3D point cloud segmentation using k-means clustering," *Traitement du Signal*, vol. 37, no. 6, pp. 1019–1027, 2020.
- [15] Q. Y. Jiang, J. X. Xie, and J. Ye, *Mathematical Model*, pp. 69–72, Higher Education Press, Beijing, China, 2003.
- [16] R. Pastor-Satorras and A. Vespignani, "Epidemic spreading in scale-free networks," *Physical Review Letters*, vol. 86, no. 14, pp. 3200–3203, 2001.
- [17] H. W. Hethcote, "The mathematics of infectious diseases," *SIAM Review*, vol. 42, no. 4, pp. 599–653, 2000.
- [18] X. Rui, F. Meng, Z. Wang, G. Yuan, and C. Du, "SPIR: the potential spreaders involved SIR model for information diffusion in social networks," *Physica A: Statistical Mechanics and Its Applications*, vol. 506, no. 9, pp. 254–269, 2018.
- [19] R. G. Zhang and G. C. Duan, "Progress in prevention and treatment of Ebola virus disease," *Journal of Xinxiang Medical University*, vol. 11, pp. 865–871, 2014.
- [20] Health Commission of Hubei Province, *Epidemic situation of Novel Coronavirus Infection in Hubei*, Health Commission of Hubei Province, Hubei, China, 2020.
- [21] P. Albrecht, "A new theoretical approach to RUNGE-KUTTA Methods," *SIAM Journal on Numerical Analysis*, vol. 24, no. 2, pp. 391–406, 1987.
- [22] X. Tang and A. Xiao, "Improved Runge-Kutta-Chebyshev methods," *Mathematics and Computers in Simulation*, vol. 174, no. 2, pp. 59–75, 2020.
- [23] Hubei Provincial Government, *General Situation of Hubei Province*, Hubei Provincial Government, Hubei, China, 2020.
- [24] C. Liao, W. S. Xu, and Q. D. Wu, "The construction and solution of large-scale emergency relief supplies of the transportation model," *Engineering*, vol. 24, no. 11, pp. 7–11, 2006.
- [25] K. Krishna and M. Narasimha Murty, "Genetic K-means algorithm," *IEEE Transactions on Systems, Man and Cybernetics, Part B (Cybernetics)*, vol. 29, no. 3, pp. 433–439, 1999.
- [26] H.-S. Park and C.-H. Jun, "A simple and fast algorithm for K-medoids clustering," *Expert Systems with Applications*, vol. 36, no. 2, pp. 3336–3341, 2009.
- [27] J. J. Xu, *Based on the Diffusion of Major Infectious Diseases Emergency Supplies Model*, Southeast University, Nanjing, China, 2011.
- [28] D. Q. Chen, *Based on the Decision Model Study of Allocation Optimization Analysis System Characteristics Emergency Supplies*, Zhejiang University, Zhejiang, China, 2010.
- [29] M. Doumpos and C. Zopounidis, "Multi-objective optimization models in finance and investments," *Journal of Global Optimization*, vol. 76, no. 2, pp. 243–244, 2020.
- [30] S. Khalfallah and H. E. Lehtihet, "A multi-objective optimization methodology based on multi-mid-range meta-models for multimodal deterministic/robust problems," *Structural and Multidisciplinary Optimization*, vol. 60, no. 6, pp. 2373–2389, 2019.
- [31] J. Liu, L. Wang, Q. Zhang, and S.-T. Yau, "The dynamical model for COVID-19 with asymptotic analysis and numerical implementations," *Applied Mathematical Modelling*, vol. 89, no. 1, pp. 1965–1982, 2021.